In-plane light particle correlations in 40 MeV/nucleon C+C, Ag, Au, and 50 MeV/nucleon C+C reactions

D. Fox, D. A. Cebra, J. Karn, C. Parks, G. D. Westfall, and W. K. Wilson
National Superconducting Cyclotron Laboratory, Michigan State University, East Lansing, Michigan 48824
(Received 5 March 1987)

Large angle correlations have been measured between two light particles ($Z=1,2$) emitted from 40 MeV/nucleon C + C, Ag, Au, and 50 MeV/nucleon C + C reactions. The first particle is detected at $\theta=-45°$, and the second particle is detected in the same plane with $-150°\leqq\theta\leqq+150°$. The correlations are consistent with emission from a thermalized system that is constrained by momentum conservation effects. In addition, the decay of particle unstable states contributes heavily to the coincidence cross sections for p-p, p-t, p-^{4}He, d-^{4}He, t-^{4}He, and ^{4}He-^{4}He correlations.

The degree to which thermalization occurs in nucleus-nucleus collisions has been studied for some time.[1-3] Both light particle and complex fragment inclusive energy spectra are thermal in appearance and come from an apparently thermalized source with a velocity intermediate between the projectile and target velocities.[3] Large angle correlations have been used to probe further the question of thermalization in nucleus-nucleus collisions. At 85 (Ref. 4) and 800 (Refs. 5–7) MeV/nucleon the relative importance of direct versus thermal phenomena has been studied by measuring the ratio of in- to out-of-plane correlations. For C + C it was shown that the correlations peak at the energies and angles corresponding to quasielastic nucleon-nucleon scattering. For a large system, C + Pb, the ratio was found to be nearly independent of angle which implied that the system was thermalized. At lower energies, 19–25 MeV/nucleon,[8-10] light systems have been found to be dominated by momentum conservation effects, while heavier systems have been shown to emit preferentially in a plane.

We have shown in the present work that light particles seem to be emitted from three thermalized sources. The three sources have projectilelike, targetlike and intermediate velocities. No evidence is seen for direct nucleon-nucleon scattering contributions.

The present experiment was conducted at the National Superconducting Cyclotron Laboratory using beams of 40 and 50 MeV/nucleon ^{12}C from the K500 Superconducting Cyclotron. The targets were 26 mg/cm^2 graphite, 4.0 mg/cm^2 Ag, and 5.5 mg/cm^2 Au. Particles were detected in ten fast-slow plastic phoswich telescopes consisting of a 1.6 mm thick fast plastic (BICRON, BC 412) ΔE detector and a 127 mm long slow plastic (BC 444) E detector. Two of the telescopes were placed in plane with $\Phi=180°$ and $\theta=25°$ and 45°. The remaining eight telescopes were placed in plane with $\Phi=0°$ and $\theta=15°$, 25°, 45°, 55°, 70°, 85°, 100°, and 150°.

The inclusive energy spectra for p, d, t, ^{3}He, and ^{4}He for 40 MeV/nucleon C + C, Ag, Au, and 50 MeV/nucleon C + C are shown in Figs. 1–4, for $\theta=15°$, 25°, 45°, 55°, 70°, 85°, 100°, and 150°. The spectra have been corrected for reaction losses in the phoswich telescopes and the errors shown are statistical. The spectra are smooth, decreasing monotonically with increasing angle and decaying exponentially at high energies, suggesting a thermal origin for the observed particles.

We have fit the data with a triple moving source parametrization, which assumes the presence of a projectilelike source, a targetlike source, and an intermediate velocity source. All three sources are assumed to move in the beam direction. While it is true that at 40–50 MeV/nucleon the three sources are not well separated, the energy spectra show definite signs of each of the three sources. The energy spectra for each source are assumed to be described by a relativistic Maxwell-Boltzmann energy distribution. In the rest frame of each source the distribution is given by

$$\frac{d^2\sigma}{p'^2dp'd\Omega'} = \frac{\sigma_0}{4\pi m^3}\frac{e^{-E'/\tau}}{2(\tau/m)^2K_1(m/\tau)+(\tau/m)K_0(m/\tau)},$$

where p' and E' are the momentum and total energy of a particle in the source rest frame, and K_0 and K_1 are modified Bessel functions of the second kind, and σ_0 and τ are the production cross section and source temperature for the given source. The energy spectra in the lab are then given by

$$\frac{d^2\sigma}{dE\,d\Omega}=\frac{pE'd^2\sigma}{p'^2dp'd\Omega'},$$

where $E'=\gamma(E-\beta p\cos\theta_{\rm lab})$, p and E are the momentum and total energy of a particle in the lab frame, $\theta_{\rm lab}$ is the lab angle, and β is the velocity of the source in the lab. For each source β, σ_0, and τ are fit by using those angles and energies that are dominated by the source being fit. For the Ag and Au targets the Coulomb shifts listed in Table I were applied prior to fitting the data. The fits are shown in Figs. 1–4 as lines and the fitted parameters are listed in Table II. The fits are excellent except for some differences at forward angles with the carbon target. The fitted parameters for the target-like source have large uncertainties due to the limited range

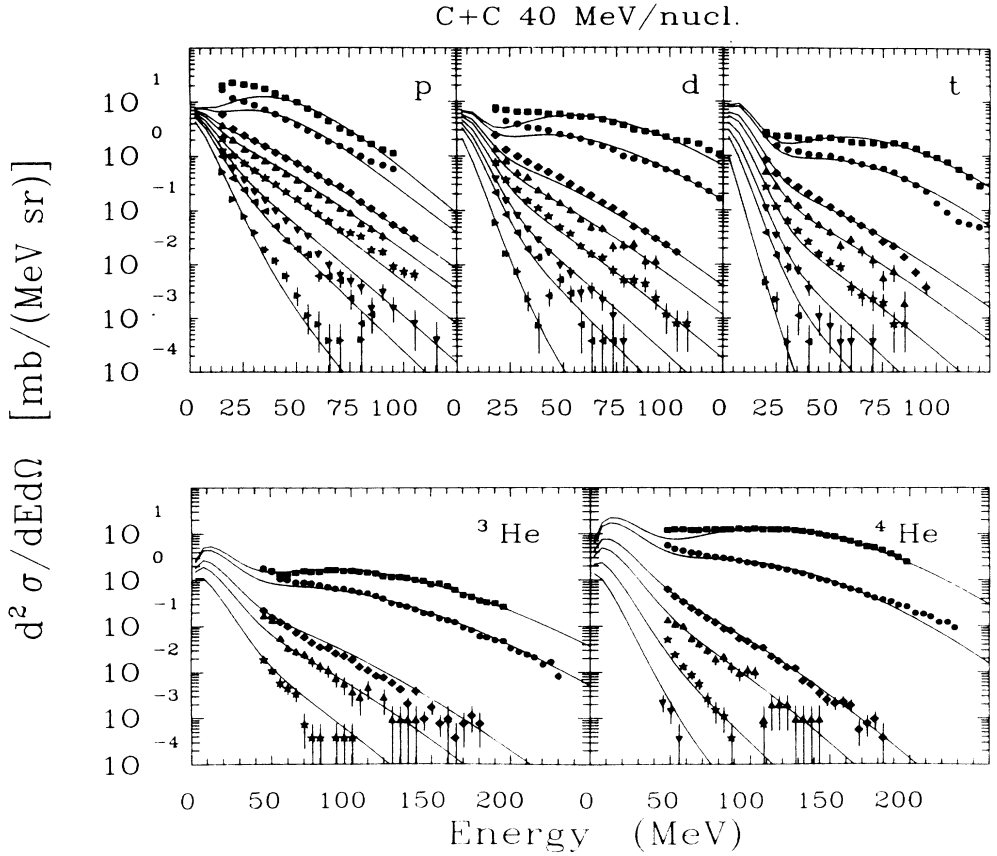

FIG. 1. Inclusive spectra for p,d,t,^{3}He,^{4}He from 40 MeV/nucleon C + C. The lines are the result of a triple moving source fit described in the text.

over which they were fitted.

The two particle correlations are shown in Figs. 5–9 for p-p, p-d, d-d, d-^{4}He, and ^{4}He-^{4}He. The correlations are shown in terms of the two particle correlation cross section, σ_{12}, divided by the singles cross sections, σ_1 and σ_2. In each case one of the particles is detected at $\theta=-45°$ and the second particle is detected between $\theta=-170°$ and $+170°$. A negative angle for the second particle means the two particles were observed on the same side of the beam, while a positive angle indicates emission on opposite sides of the beam. For the nonidentical particle cases (p-d, d-^{4}He), the case where the heavier particle was detected at $\theta=-45°$ is shown. The energy ranges over which the coincidences were integrated are given in Table III.

In general the correlations for the C + C systems show a broad maximum at positive angles indicating a preference for emission on opposite sides of the beam. The magnitude of the peak increases as the mass of the observed particles increase. For negative angles the general trend is that the correlations do not change much with angle. The p-p and d-^{4}He correlations are exceptions to this trend because they show peaks at $\theta=-55°$. These peaks come from the decay of particle unstable states in ^{2}He and ^{6}Li. The C + Ag and C + Au systems have different systematic behavior. The correlation function is in general almost symmetric about $\theta=0°$ with the same side being only slightly preferred. The p-p peak coming from ^{2}He break up in the light C + C systems is considerably weaker in the heavier systems. Both the d-^{4}He and ^{4}He-^{4}He correlations show strong peaks coming from the decay of particle unstable states of ^{6}Li and ^{8}Be. The ^{4}He-^{4}He peak was not observed in the lighter systems because it is difficult to form a ^{8}Be given that the average intermediate velocity source contains only 12 nucleons. The particle pairs that are not shown all exhibit the same characteristics that are seen in Figs. 5–9. The p-t, p-^{4}He, and t-^{4}He correlations all have peaks at $\theta=-55°$ coming from the decay of particle unstable states.

TABLE I. Coulomb shifts used for the moving source fits for the Ag and Au targets.

Target	Particle	V_C (MeV)
Ag	p,d,t	4
Ag	^{3}He,^{4}He	8
Au	p,d,t	5
Au	^{3}He,^{4}He	10

Energy and momentum conservation effects have been used to explain the observed correlations for small systems at lower energies.[9,10] In order to explore the extent to which our data is affected by conservation laws we have carried out calculations incorporating these effects. The calculation assumes emission of two particles from a source of size A. After the first particle is emitted the

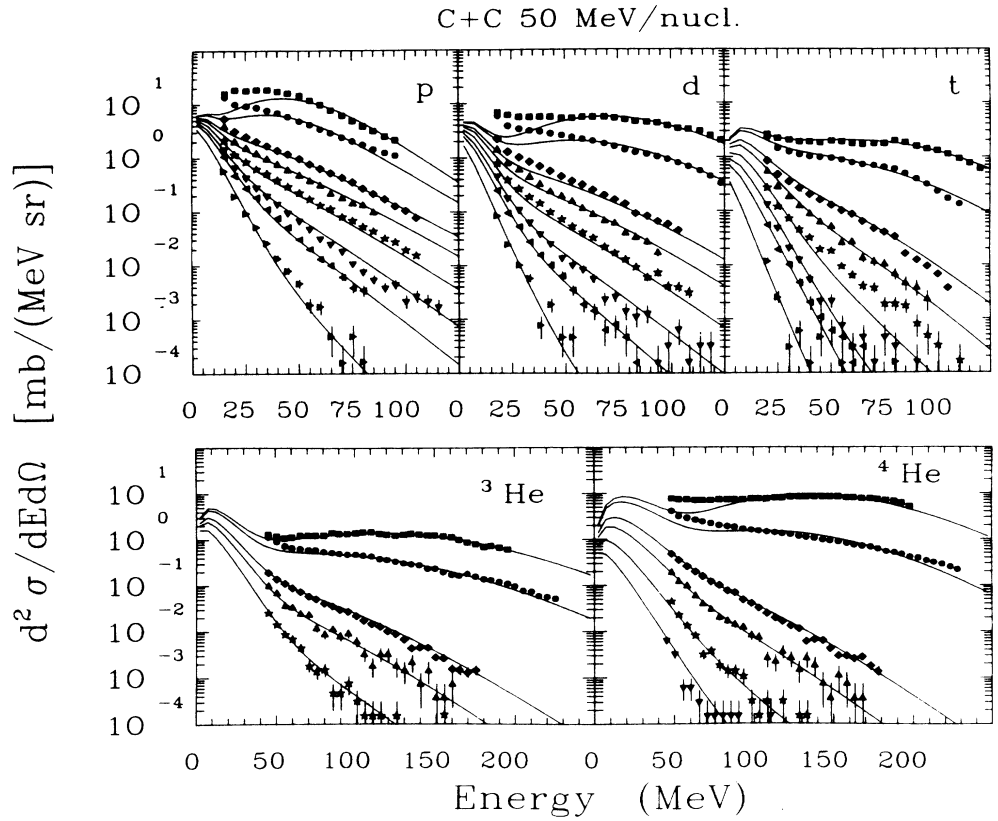

FIG. 2. Inclusive spectra for p,d,t,^{3}He,^{4}He from 50 MeV/nucleon C + C. The lines are the result of a triple moving source fit described in the text.

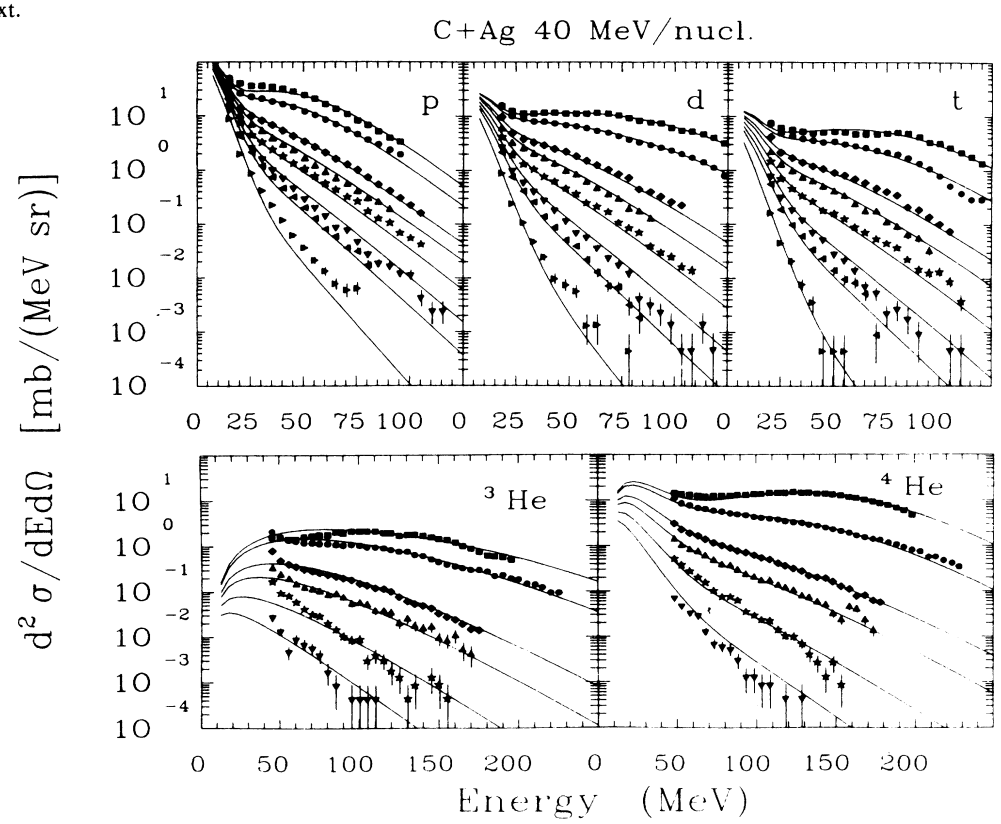

FIG. 3. Inclusive spectra for p,d,t,^{3}He,^{4}He from 40 MeV/nucleon C + Ag. The lines are the result of a triple moving source fit described in the text.

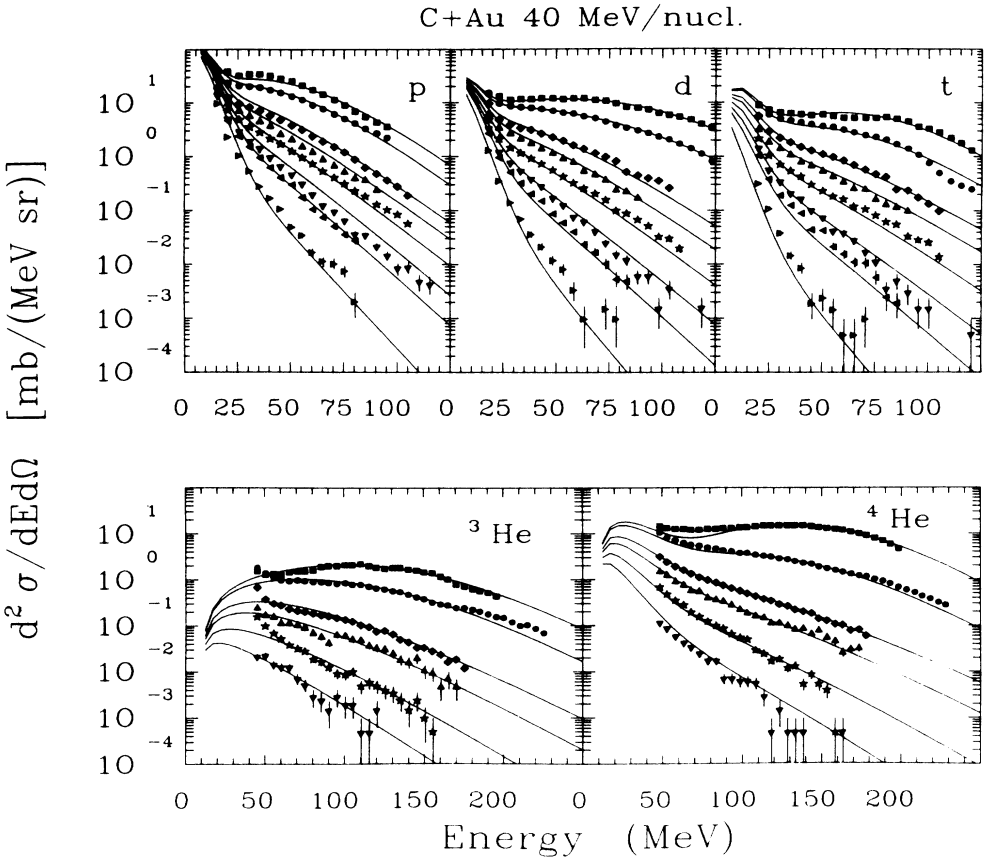

FIG. 4. Inclusive spectra for p,d,t,^{3}He,^{4}He from 40 MeV/nucleon C + Au. The lines are the result of a triple moving source fit described in the text.

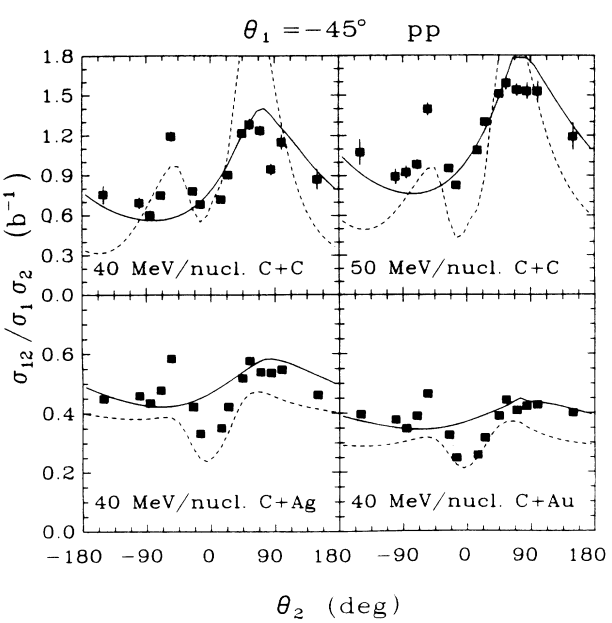

FIG. 5. Two proton correlation function where one proton is detected at $\theta = -45°$. The lines are the results of momentum conservation calculations that are described in the text.

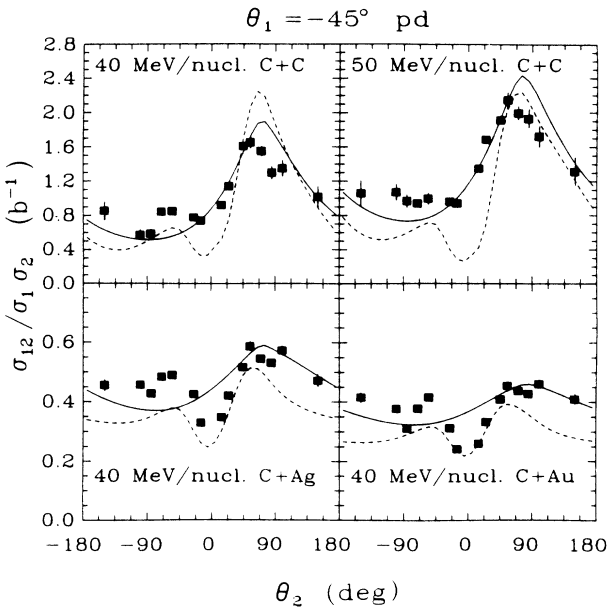

FIG. 6. Proton-deuteron correlation function where the deuteron is detected at $\theta = -45°$. The lines are the results of momentum conservation calculations that are described in the text.

TABLE II. Moving source parameters for the targetlike, intermediate velocity, and projectilelike sources. The targetlike source was not fit for the Ag and Au targets.

	Targetlike source			Intermediate source			Projectilelike source		
Particle	Cross section σ_0 (mb)	Velocity β	Temperature τ (MeV)	Cross section σ_0 (mb)	Velocity β	Temperature τ (MeV)	Cross section σ_0 (mb)	Velocity β	Temperature τ (MeV)
				40 MeV/nucleon C + C					
p	620	0.016	4.58	472	0.146	11.37	311	0.259	4.90
d	471	0.027	4.29	138	0.124	11.09	215	0.234	5.46
t	464	0.037	3.82	56	0.124	10.28	74	0.201	5.73
^{3}He	284	0.064	5.50	62	0.152	11.78	95	0.251	9.56
^{4}He	971	0.071	5.31	256	0.149	9.70	757	0.240	6.98
				50 MeV/nucleon C + C					
p	603	0.022	5.30	460	0.174	14.02	361	0.288	5.17
d	375	0.026	4.84	158	0.145	13.00	239	0.267	6.56
t	205	0.047	5.51	99	0.153	8.77	51	0.237	5.50
^{3}He	354	0.053	6.18	60	0.184	12.67	90	0.291	9.87
^{4}He	472	0.080	6.79	111	0.165	11.68	652	0.271	7.89
				40 MeV/nucleon C + Ag					
p	8226	0.015	3.53	1912	0.129	11.91	758	0.257	6.12
d	1827	0.019	4.16	915	0.123	11.87	411	0.251	7.75
t	795	0.020	4.16	416	0.113	11.74	157	0.210	6.20
^{3}He				241	0.179	15.36	66	0.278	11.42
^{4}He	1640	0.063	6.98	808	0.163	15.96	737	0.255	7.03
				40 MeV/nucleon C + Au					
p	8699	0.012	3.61	2448	0.123	12.16	667	0.263	6.72
d	2014	0.015	3.81	1025	0.118	12.16	414	0.256	7.49
t	1097	0.031	4.25	476	0.115	13.26	154	0.208	5.29
^{3}He				162	0.168	17.13	88	0.267	8.69
^{4}He	1246	0.069	7.69	569	0.154	18.40	866	0.253	6.57

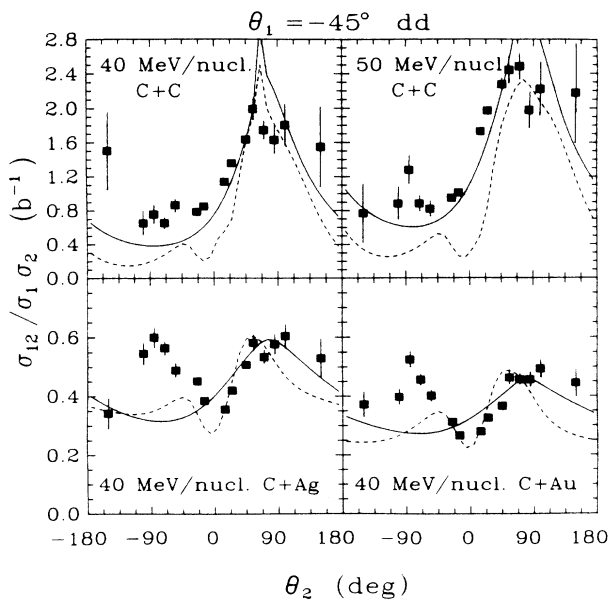

FIG. 7. Two deuteron correlation function where one deuteron is detected at $\theta = -45°$. The lines are the results of momentum conservation calculations that are described in the text.

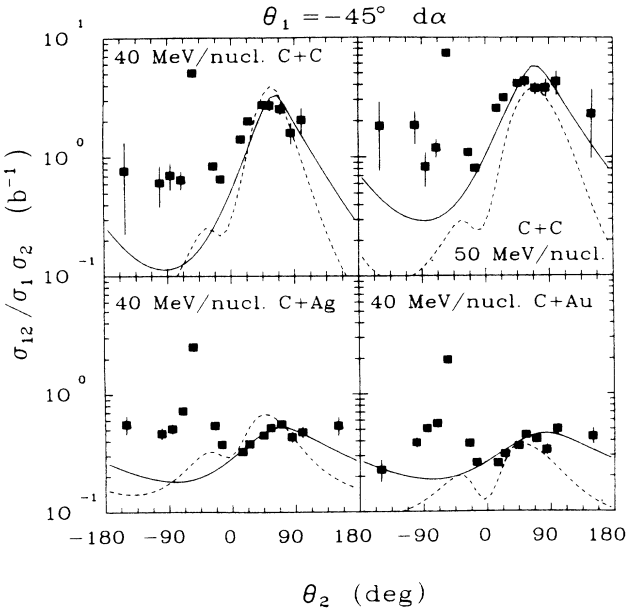

FIG. 8. Deuteron-^{4}He correlation function where the alpha is detected at $\theta = -45°$. The lines are the results of momentum conservation calculations that are described in the text.

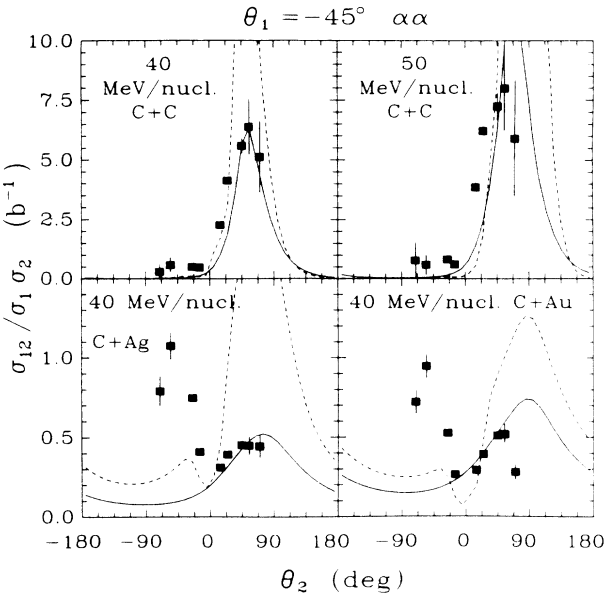

FIG. 9. Two ^{4}He correlation function where one ^{4}He is detected at $\theta = -45°$. The lines are the results of momentum conservation calculations that are described in the text.

source recoils, reequilibrates, and then emits the second particle. The calculation is repeated with the second particle being emitted first. The two cases are then averaged to produce the final coincidence cross section. The entire calculation is integrated over impact parameter with each impact parameter having a weight $W = 2\pi b\, db\, A$ where b is the impact parameter and A is the source size which comes from a fireball model[11] calculation. The calculation is normalized by the total reaction cross section. The parameters listed in Table II for the intermediate source were used to describe the emitting source.

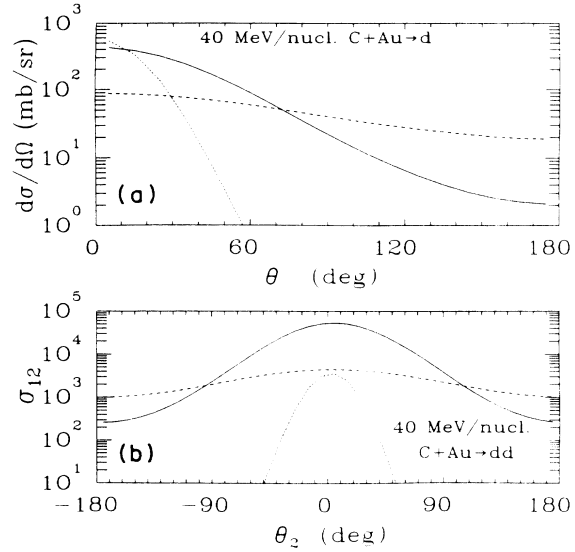

FIG. 10. Contributions to the deuteron singles cross section and the two deuteron coincidence cross section for 40 MeV/nucleon C + Au from the projectilelike source (dotted line), intermediate source (solid line), and targetlike source (dashed line).

TABLE III. Energy ranges integrated over for the two particle correlations.

Particle	Energy (MeV)
p	12–80
d	16–80
^{4}He	47–135

The results of the momentum conservation calculations are shown in Figs. 5–9 as solid lines. The calculations have been renormalized to the data at $\theta = +45°$ and $+55°$. The calculations do a good job of reproducing the general trends in the data, but miss some of the details. In the lighter systems the same side correlations are basically flat, except for those cases that have contributions from the decay of resonances, while the calculation predicts a broad minimum at about $\theta = -80°$. The heavier systems have a "V" shaped dip around $\theta = 0°$, but the calculations show no such dip.

Until now we have assumed that the observed two particle correlations are coming only from the intermediate source although from the inclusive spectra shown in Figs. 1–4 it is evident that a substantial fraction of the observed particles come from sources other than the intermediate source. In Fig. 10(a) the contribution to the deuteron singles cross section from each of the three observed sources is shown for C + Au system. For small angles the projectile source contributes heavily to the singles cross section, while for large angles the targetlike source dominates the cross section. Even for small angles where one would expect the projectilelike source to dominate, the targetlike source contributes about 10% of the total cross section. Figure 10(b) shows the contribution to the two deuteron coincidence cross section from each of the three sources according to momentum conservation calculations using the parameter for each of the sources given in Table II. From Fig. 10(b) we can see that adding the contributions of the three sources together will increase the coincidence cross section around $\theta = 0°$ by less than 10% while in Fig. 10(a) we see that the addition of the projectile and targetlike sources more than doubles the singles cross sections near $\theta = 0°$. This summation will lead to the dip around 0° which is observed in the data.

The dashed lines in Figs. 5–9 are the results of three source momentum conservation calculations. These calculations take into account only correlations between two particles coming from the same source. Unlike the single source calculation discussed earlier, no normalization has been applied to the three source calculation. The calculation now produces a "V" shape for small θ for the heavier systems. Also where the single source calculation had a broad minimum for same side correlations, the three source calculation shows a maximum at about $\theta = -55°$. This maximum is almost as large as the opposite side maximum for the heavier systems. The most

notable disagreement between the data and the three source calculation is the underprediction of the coincident cross section for large θ. This disagreement is probably due to correlations between particles that come from different sources which are not included in the calculation.

In conclusion we have found that for both light and heavy systems momentum conservation effects seem to account for the gross features of two particle correlations if one considers all the sources that are present. By taking into account contributions from the targetlike and projectilelike sources the momentum conservation calculation predicts the "V" shaped dip at small angles previously attributed to emission from a rotating ideal gas.[10] Large angle correlations on the same side of the beam show strong contributions from the break up of particle unstable resonances.

This work was supported by the National Science Foundation under Grant No. PHY-86-11210.

[1]T. C. Awes, S. Saini, G. Poggi, C. K. Gelbke, D. Cha, R. Legrain, G. D. Westfall, Phys. Rev. C **25**, 2361 (1982).

[2]G. D. Westfall, B. V. Jacak, N. Anantaraman, M. V. Curtin, G. M. Crawley, C. K. Gelbke, B. Hasselquist, W. G. Lynch, D. K. Scott, M. B. Tsang, M. J. Murphy, T. J. M. Symons, R. Legrain, and T. J. Majors, Phys. Lett. **116B**, 118 (1982).

[3]B. V. Jacak, G. D. Westfall, C. K. Gelbke, L. H. Harwood, W. G. Lynch, D. K. Scott, H. Stöcker, M. B. Tsang, and T. J. M. Symons, Phys. Rev. Lett. **51**, 1846 (1983).

[4]P. Kristiansson, L. Carlen, H.-Å. Gustafsson, B. Jakobsson, A. Oskarsson, H. Ryde, J. P. Bondorf, O.-B. Nielsen, G. Lovhoiden, T.-F. Thorsteinsen, D. Heuer, and H. Nifenecker, Phys. Lett. **155B**, 31 (1985).

[5]S. Nagamiya, L. Anderson, W. Bruckner, O. Chamberlain, M.-C. Lemaire, S. Schnetzer, G. Shapiro, H. Steiner, and I. Tanihata, Phys. Lett. **81B**, 147 (1979).

[6]I. Tanihata, M.-C. Lemaire, S. Nagamiya, and S. Schnetzer, Phys. Lett. **97B**, 363 (1980).

[7]I. Tanihata, S. Nagamiya, S. Schnetzer, and H. Steiner, Phys. Lett. **100B**, 121 (1981).

[8]W. G. Lynch, L. W. Richardson, M. B. Tsang, R. E. Ellis, C. K. Gelbke, and R. E. Warner, Phys. Lett. **108B**, 274 (1982).

[9]M. B. Tsang, W. G. Lynch, C. B. Chitwood, D. Fields, D. R. Klesch, C. K. Gelbke, G. R. Young, T. C. Awes, R. L. Ferguson, F. E. Obenshain, F. Plasil, and R. L. Robinson, Phys. Lett. **148B**, 265 (1984).

[10]C. B. Chitwood, D. J. Fields, C. K. Gelbke, D. R. Klesch, W. G. Lynch, M. B. Tsang, T. C. Awes, R. L. Ferguson, F. E. Obenshain, F. Plasil, R. L. Robinson, and G. R. Young, Phys. Rev. C **34**, 858 (1986).

[11]J. Gosset, H. H. Gutbrod, W. G. Meyer, A. M. Poskanzer, A. Sandoval, R. Stock, and G. D. Westfall, Phys. Rev. C **16**, 629 (1977); G. D. Westfall, J. Gosset, P. J. Johansen, A. M. Poskanzer, W. G. Meyer, H. H. Gutbrod, A. Sandoval, and R. Stock, Phys. Rev. Lett. **37**, 1202 (1976).